Augmented Reality and UWB Technology Fusion: Localization of Objects with Head-Mounted Displays

Francisco Molina Martel, *Fraunhofer-Institut für Optronik, Systemtechnik und Bildauswertung*
Juri Sidorenko
Christoph Bodensteiner
Michael Arens

BIOGRAPHIES

Francisco Molina Martel received his Bachelor degree in Energy and Automation Technology from Karlsruhe University of Applied Sciences and graduated with a Master of Science Degree in Embedded Systems at Pforzheim University in 2011 and 2014. On 2014 he joined the Adaptive Optics group at Fraunhofer IOSB in Ettlingen, Germany. Since August 2017 he is working in the group Object Recognition in Sensor Networks at the same institute, where he is researching in the field related to integration of ultra-wideband technology in visual SLAM based Augmented Reality devices.

Juri Sidorenko received the diploma in mechanical engineering from the Technical University Braunschweig, Germany and the Master of Science from the Cranfield University, UK in 2012 and 2014.

Christoph Bodensteiner received the M.S. degree in computer science from the Technical University Munich, Germany and the Ph.D. degree at the Institute for Robotics at the University of Lübeck, Lübeck, Germany. He was a Software Engineer developing systems for surgical navigation and is currently heading a research group at the Fraunhofer IOSB. His research interests include (non)-rigid 2-D/3-D registration, vision based localization and 3-D reconstruction in medical and remote sensing applications.

Dr. Michael Arens received his diploma in Computer Science and his PhD (Dr.rer.nat) from the University of Karlsruhe in 2001 and 2004, respectively. Since 2006, he works at the Fraunhofer Institute of Optronics, System Technologies and Image Exploitation in various positions. In 2011 Dr. Arens was appointed Head of the Department of Object Recognition. His research interests include image and video analysis with an emphasis on the automatic conceptualization and reasoning on results obtained from such an analysis where he has co-authored several articles. Dr. Arens has participated in the EU-project CogViSys-Cognitive Vision Systems from 2001 until 2004. He is member of the German Association of Pattern Recognition (DAGM) and member of the IEEE.

ABSTRACT

Technical advances in computer vision, visual inertial odometry and display technology in the past years have produced a considerable improvement in Augmented Reality (AR). However, none of the contemporary commercial Head-Mounted Displays (HMDs) locates objects that are not in direct line-of-sight with a camera. Our objective is the localization of unseen objects and their visualization through an AR HMD. We extend the functionality of an AR HMD by integrating an ultra-wideband (UWB) transceiver on a Microsoft HoloLens. The UWB transceiver estimates the distance to another UWB transceiver via time of arrival.

For UWB ranging, two different protocols have been proposed by the IEEE 802.15.4a-2007 standard: Two-Way Ranging (TWR) and Symmetric Double-Sided Two-Way Ranging (SDS-TWR). In this work we consider three different TWR implementations and the standard SDS-TWR method. Two of the three implemented TWR methods use a DecaWave DW1000 IC utility for estimating the clock frequency offset. Our method processes this data with a digital low-pass filter in order to remove the fluctuations induced by the frequency offset estimation error.

We localize a static UWB transponder with trilateration, given the measured distance and the calculated positions of the integrated UWB antenna in the HoloLens coordinate frame. We measure and compare the accuracy and precision achieved with three different implemented TWR ranging methods and SDS-TWR. The precision achieved with our TWR method even surpasses SDS-TWR in our measurements. We localize and visualize the estimated position of the UWB transceiver in the HMD with an accuracy of 6 cm for position dilution of precision (PDOP) values smaller than 10.

I. INTRODUCTION

A considerable amount of research has been done in the field of indoor localization and mapping since a few decades and Augmented Reality (AR) has notably benefited from advances in this field. A good example is the Microsoft HoloLens, a pair of AR smartglasses that are available since March of 2016. In order to achieve realistic 3D projection rendering, the device has to orient itself in its environment. It applies Visual Inertial Odometry (VIO) and Simultaneous Localization and Mapping (SLAM) techniques. That is, the system has to concurrently map the surrounding three-dimensional space and estimate its own pose (position and orientation) relative to the constructed map.

No commercial AR Head-Mounted Display (HMD) provides the ability to localize and visualize objects that remain outside of the field of view. For this reason we have extended the AR device functionality, integrating an ultra-wideband (UWB) transceiver on the HoloLens. The UWB transceiver uses time of arrival (TOA) technique to measure the distance to another UWB transceiver. Then it sends this distance data over WLAN connection to the smartglasses.

Another advantage of using UWB technology is the resilient localization of several smartglasses under harsh conditions (low lighting, smoke, dust) or in the absence of a loop closure, where cooperative SLAM based visual odometry would fail.

We focus at locating one UWB transceiver placed at a random position with a HoloLens and a second UWB transceiver attached to it. In the following subsections we introduce the localization systems used in this paper.

A. Visual Inertial Odometry (VIO)

The HoloLens performs real-time Visual Inertial Odometry (VIO) with following integrated sensors: an inertial measurement unit (IMU), four RGB-cameras and an energy-efficient depth camera. Real-time and accurate pose estimation is essential for augmented reality (AR) applications. The resulting pose estimation of the HoloLens has been verified to be very precise [4].

B. UWB technology for indoor localization

The ultra-wideband (UWB) technology is a wireless telecommunication system, which is less sensitive as other technologies to reflections and multipath propagation. It is well suited for indoor and GPS denied applications. We use the DecaWave EVB1000 evaluation boards. Each transceiver contains a STM32F105 ARM Cortex M3 processor and a DW1000 RF integrated chip.

C. Optical systems – HTC Vive infrared localization

The HTC Vive is a VR HMD that uses an optical tracking technology. This enables a precise tracking of the HMD and controllers at millimeter level. Each mobile unit is equipped with an IMU and several infrared photodiodes. Because of its high precision, we use its measurements as the ground truth reference for result evaluation. The used tracking space has the size of 4 x 3 meters and the infrared emitters were placed approximately at a height of 2.40 meters.

Related Work

Several asynchronous ranging protocols have been proposed. In [8] Two Way Ranging (TWR) and Symmetric Double-Sided Two-Way Ranging (SDS-TWR) are considered. Several works [14], [12], [5] choose TWR, because less messages have to be exchanged between nodes. All of these mentioned papers estimate the clock skew and correct the clock drift error induced by TWR. The works in [12], [14] use the DW1000 IC functionality for estimating the clock frequency offset. The authors in [5] propose using the timestamps of previous ranging messages in order to estimate the clock skew with linear regression.

Contributions

We propose a novel method for clock skew estimation with the DW1000 IC utility. We extend the estimation with a low-pass filter, improving the UWB ranging precision of [12] and [14]. We show how to combine an UWB system with a HMD-AR system and localize a static UWB transceiver in the HMD coordinate frame. We provide an accuracy and precision analysis using this combined localization system.

Outline

Section II is divided in two parts: II-A describes the TWR and SDS-TWR ranging protocols, their respective errors and our implemented TWR methods with clock drift compensation. Section II-B illustrates how to localize an UWB transceiver with AR smartglasses. Section III specifies the accuracy and precision of the different implemented UWB ranging methods and of the whole localization system.

II. METHODS

A. Ultra-wideband

1.) Ranging protocols

When two transceivers share perfect clock synchronization a single-way message is sufficient for the receiver in order to estimate the time of flight (TOF). In the absence of clock synchronization, more than one message is required. In the IEEE 802.15.4a-2007 standard [8] two ranging protocols for asynchronous ranging are proposed: Two-Way Ranging (TWR) and Symmetric Double-Sided Two-Way Ranging (SDS-TWR).

TWR uses two messages and SDS-TWR improves accuracy at the expense of having to exchange a total of three messages. The functionality of both protocols is illustrated in figure 1. By timestamping the exact moment of the transmitted and received signals in both nodes it is possible to estimate the time of flight (TOF).

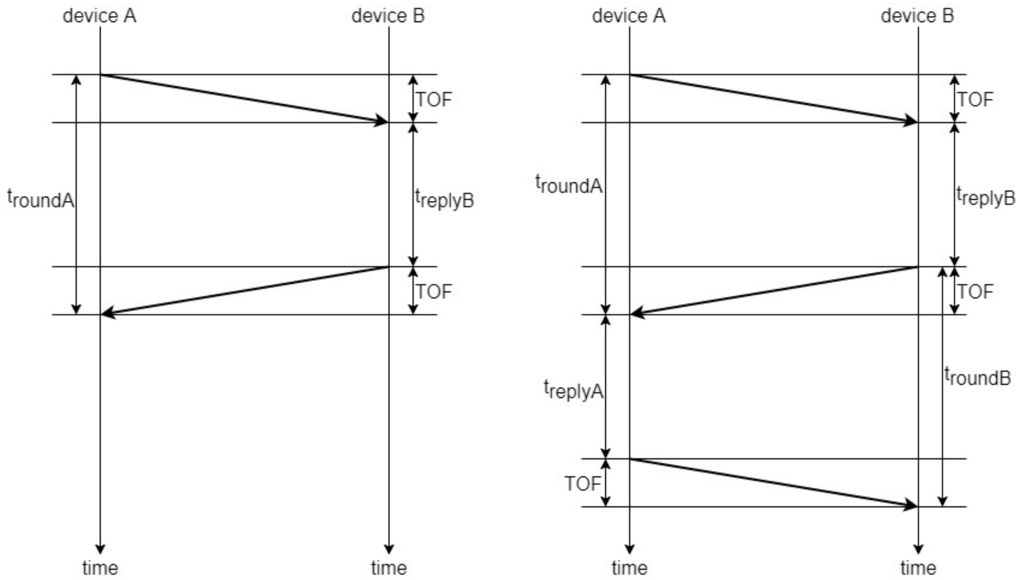

(a) Two-Way Ranging (b) SDS-TWR

Figure 1: TWR and SDS-TWR.

In the case of TWR we can observe in figure 1 that the TOF can be calculated as follows:

$$TOF = \frac{1}{2}\left[t_{roundA} - t_{replyB}\right] \tag{1}$$

But in practice, due to the clock drift effects we can only measure the estimates of the time

$$\hat{t}_{roundA} = (1 + e_A)t_{roundA} \tag{2}$$
$$\hat{t}_{replyB} = (1 + e_B)t_{replyB} \tag{3}$$

where e_A and e_B represent the frequency error offset from the nominal frequency and are expressed in parts per million (ppm). The estimated time of flight $T\hat{O}F$ results in equation (4).

$$T\hat{O}F = \frac{1}{2}\left[\hat{t}_{roundA} - \hat{t}_{replyB}\right] \tag{4}$$

As expressed in [8], [3] the standard TWR method has an approximate error of

$$e = T\hat{O}F - TOF \approx \frac{1}{2}\left[t_{replyB}(e_A - e_B)\right] \quad (5)$$

SDS-TWR compensates the error of the TWR protocol using the symmetry of two TWR message exchanges, trying to minimize the time difference $\Delta t_{reply} = t_{replyB} - t_{replyA}$ given that the error in this case is equal to

$$e \approx \frac{1}{4}\Delta t_{reply}(e_A - e_B) \quad (6)$$

The interested reader might find further information about SDS-TWR in [8] and [3].

2.) TWR Clock Drift Compensation (TWR-CDC)

Similarly to [12] and [14] we use a DW1000 chip functionality, which estimates the clock frequency difference between both transceivers in ppm. We correct the estimated time of flight of TWR in equation (4) by reading the estimated frequency offset $\Delta\hat{e}_k$ after the frame transmission and applying equation (7).

$$T\hat{O}F_{corrected} = T\hat{O}F - \frac{1}{2}\left[\hat{t}_{replyB}\Delta\hat{e}_k\right] \quad (7)$$

The resulting error reduces to equation (8) and largely depends on how accurate the clock offset estimation $\Delta\hat{e}_k$ is.

$$e \approx \frac{1}{2}\left[t_{replyB}(e_A - e_B) - (1 + e_B)t_{replyB}\Delta\hat{e}_k\right] \quad (8)$$

In addition to [14], [12] and [5], we also consider the fluctuation of the clock frequency offset estimate $\Delta\hat{e}_k$. It fluctuates with an approximate standard deviation σ = 0.16 ppm. Assuming a typical room temperature crystal oscillator (RTXO) short-term stability in the order of $2 \cdot 10^{-9}$ [7], this fluctuation is dominantly induced by estimation error. This error affects the variance of the TOF estimation and thus degrades the precision of the UWB ranging.

3.) TWR low-pass filtered Clock Drift Compensation (TWR-LPF-CDC)

We use a single-pole low-pass IIR filter to reduce the fluctuations of the clock frequency offset estimations $\Delta\hat{e}_k$. The filter is described in equation (9), where the parameter $\alpha \in \mathbb{R}$ with $0 < \alpha < 1$ for a low-pass filter effect. The IIR filter is stable as long as the condition $| 1-\alpha | < 1$ is satisfied.
We chose a small value of $\alpha = 0.01$ in order to mitigate these fluctuations as much as possible. This value was determined empirically. We insert the filtered value $\hat{x}_k$ into equation (7) as the frequency offset estimate.

$$\hat{x}_k = \hat{x}_{k-1} + \alpha(\Delta\hat{e}_k - \hat{x}_{k-1}) \quad (9)$$

4.) Further UWB error sources

Although the DW1000 IC computes a leading edge detection algorithm [1], the measured distances still have a bias error [3]. This error depends on the received signal level. When the received signal level is weak, the measured distance is up to ten centimeter larger than ideal and vice versa.
In order to correct for this error we performed distance measurements in the range between zero and ten meters. The ground truth distance was determined with a laser distance measurer pointing from antenna to antenna. In this range below 10 meter the measured distances have shown a linear tendency, so that the UWB distance measurements can be fitted to the following linear function:

$$f(x) = 0.969 \cdot x + 0.0979m \quad (10)$$

This simple correction based on the measured distance is only valid in line-of-sight (LOS) situations, since non-line-of-sight (NLOS) attenuates the received signal power. NLOS identification and mitigation can be applied as in [6], [10], [15], [2], [13], [9].

B. Localization

An UWB transponder is mounted on the smartglasses as shown in figure 2. The HoloLens pinpoints the other transponder and visualizes its location. We assume that the position of the UWB device to be localized is stationary. We estimate the unknown position of the static UWB transponder *s*. The euclidian distance between the UWB antenna a_i, mounted on the HoloLens, and the static UWB device should be the same as the measured distance d_i. We assume gaussian noise distribution as shown in figure 3, so we apply a least squares solution.

$$\arg\min_{s} \sum_{i=0}^{N} f_i^2(s) \coloneqq \arg\min_{s} \sum_{i=0}^{N} (\|s - a_i\|_2 - d_i)^2 \qquad (11)$$

The position of the UWB antenna on the HoloLens a_i is given by equation (12).

$$a_i = a_i^{HL} + R_i^{HL} \vec{x}_{shift} = \begin{pmatrix} x_i \\ y_i \\ z_i \end{pmatrix} \qquad (12)$$

With a_i^{HL} as the HoloLens position and R_i^{HL} the rotation matrix, which derives from the given HoloLens euler angles (yaw, pitch, roll). The spatial offset between the local physical origin of the HoloLens and the mounted UWB antenna is defined by $\vec{x}_{shift}$. This is also illustrated in figure 2.

Given that the local origin of the HoloLens is unknown, we cannot measure the offset $\vec{x}_{shift}$ directly. It is possible to put the offset $\vec{x}_{shift}$ as another unknown in equation (11) and estimate it along the searched position *s*. However it is more precise to calculate this offset once thoroughly and accurately. Assuming that the antenna is fixed permanently onto the smartglasses, this calibration has to be performed only once. The measurement of the antenna-offset is explained in the following subsection.

We apply the Levenberg-Marquardt algorithm [11] to equation (11) as it has been proven effective for solving other similar minimization problems [16]. We input the following Jacobian matrix into the algorithm in order to make it more robust and improve its performance.

$$J_f = \left(\begin{bmatrix} \frac{x - x_1}{\|s - a_1\|_2} & \frac{y - y_1}{\|s - a_1\|_2} & \frac{z - z_1}{\|s - a_1\|_2} \\ \vdots & \ddots & \vdots \\ \frac{x - x_N}{\|s - a_N\|_2} & \frac{y - y_N}{\|s - a_N\|_2} & \frac{z - z_N}{\|s - a_N\|_2} \end{bmatrix} \right) \qquad (13)$$

1.) Calibration of the antenna-offset

In order to estimate the antenna-offset, we use the HTC Vive tracking technology. We fix a HTC Vive tracker at the same position as the mounted UWB antenna. The Vive tracker a_i^{HTC} resides in a coordinate frame, which differs from the HoloLens coordinate frame. For that reason the tracker positions in the HTC Vive coordinate system have to be transformed into the HoloLens coordinate frame with a rotation R_α and a translation $\vec{b}$.

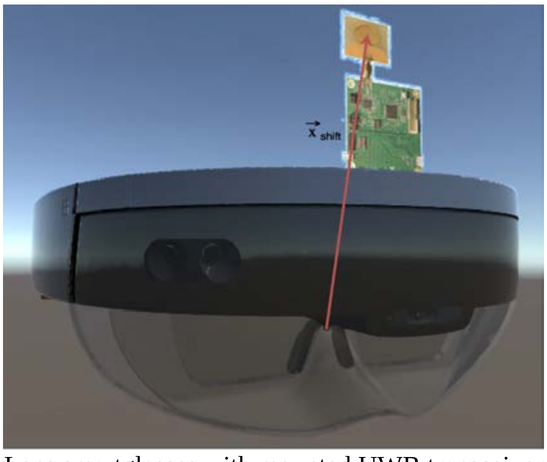

Figure 2: HoloLens smartglasses with mounted UWB transceiver (DW1000 IC)

We assume that the HTC Vive system and the HoloLens IMU are sufficiently precise for a correct vertical axis alignment and scale of the two different coordinate frames. The rotation R_α is then an elementary rotation with the angle α around the vertical axis. The offset $\vec{x}_{shift}$ can be calculated in equation (14), with given positions a_i^{HL} and rotations R_i^{HL} of the HoloLens.

$$R_\alpha a_i^{HTC} + \vec{b} = a_i^{HL} + R_i^{HL} \vec{x}_{shift} \tag{14}$$

III. RESULTS

A. Ultra-wideband

1.) UWB distance Precision and Accuracy

We compare the mean error and the standard deviation of different implemented methods. Each method was measured 5000 times at a ground truth distance of 1 meter. The resulting mean error and standard deviation were then calculated. Due to other induced errors such as bad antenna delay calibration, there still exists a remaining large bias error of more than 15 cm. The method with best precision measured was TWR-LPF-CDC. This method resulted in a standard deviation of 1.77 cm and a mean error of 18.06 cm. The distribution function is shown in figure 3.

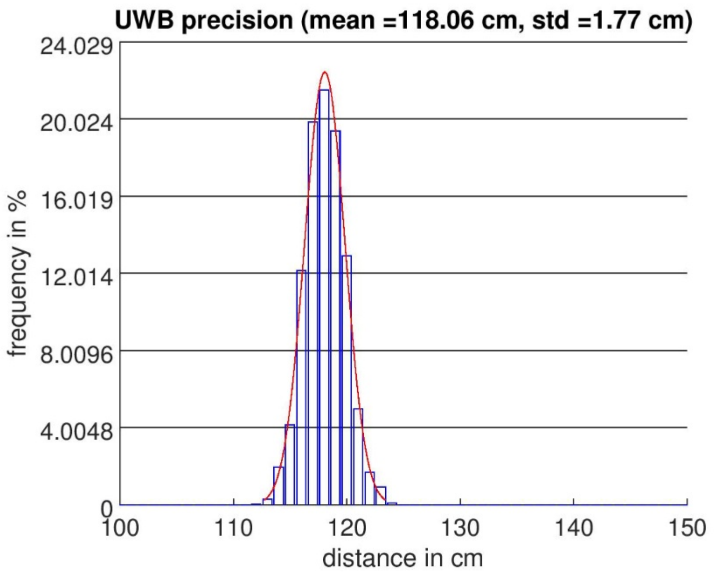

Figure 3: Measured probability distribution with two DW1000 IC transponders at a ground truth distance of 1 meter using TWR-LPF-CDC

Table I shows the measured mean error and standard deviation of the three different implemented TWR methods and SDS-TWR.

Table I: Mean error and std. deviation of the different Two-Way Ranging (TWR) methods

Ranging method	**Mean error**	**Std. deviation**
TWR	29.90 cm	1.91 cm
TWR-CDC	16.91 cm	2.23 cm
TWR-LPF-CDC	18.06 cm	1.77 cm
SDS-TWR	14.52 cm	2.08 cm

B. Localization

1.) Localization Precision and Accuracy

For each distance measured with the UWB device we read the pose of the HoloLens and calculate the position of the antenna with equation (12). After a fixed number of measurements we locate the static UWB transceiver using equation (11). In figure 4 we show the path of the integrated antenna. Each colored path represents a set of 50 antenna positions and the respective localization is illustrated as circles of the same color. The black bigger circle represents the ground truth position of the static UWB transceiver.

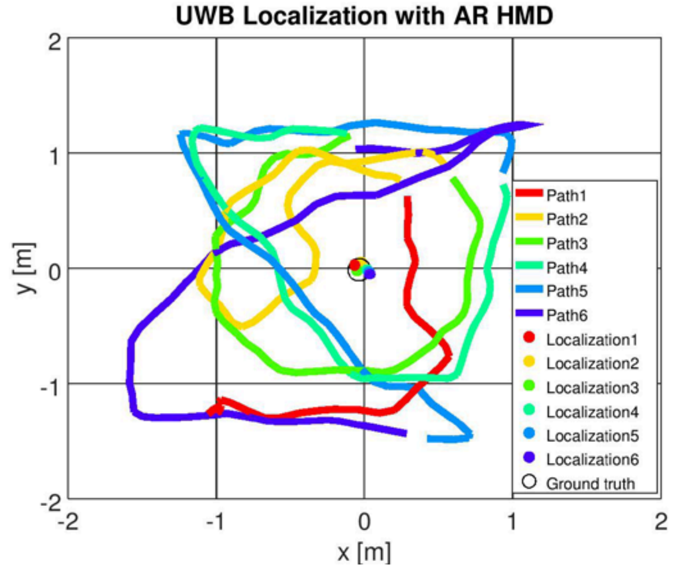

Figure 4: Measured path of the mounted antenna and estimated positions

We also calculate the positional, vertical and horizontal dilution of precision (PDOP, VDOP, HDOP). If PDOP is too high, then the localization process can be discarded for the current set. In **table II** we list the accuracy achieved in figure 4 and the calculated DOP values. The shown accuracy is the threedimensional distance between the estimated position of the transceiver and the ground truth position measured by the optical system.

Table II: DOP values and accuracy achieved for each set of 50 measurements

Path	Accuracy	PDOP	HDOP	VDOP
1	5.58 cm	2.81	0.90	2.66
2	6.81 cm	1.62	0.75	1.44
3	1.70 cm	5.95	0.49	5.93
4	5.81 cm	1.86	0.43	1.81
5	8.71 cm	1.42	0.42	1.36
6	9.71 cm	1.76	0.55	1.68

We repeated this experiment five times achieving similar results. The mean localization accuracy is 6 cm and the localization standard deviation results in 3.3 cm.

IV. CONCLUSIONS

We combine a modern AR HMD with UWB transceivers to localize and visualize objects in the coordinate frame of the smartglasses. We use a simple but effective digital low-pass filter to dampen fluctuations in clock skew estimation and correct the TWR error of equation (5). The used method achieves a mean error of 18.06 cm and a precision with a standard deviation of 1.77 cm, improving the ranging precision of 2.23 cm achieved with the method used in [12] and [14]. The accuracy is close to SDS-TWR and the precision is at least as good as SDS-TWR. Due to less message exchanges in TWR, the update rate can be increased by 50% or energy consumption can be reduced. We localize and visualize an approximate position estimation in the HMD with a mean accuracy of 6 cm and a standard deviation of 3.3 cm for PDOP values smaller than 10. In ongoing work we will further study localization problems with several AR HMDs with integrated UWB transceivers. Several UWB transceivers might be useful in order to trilaterate the position of the sought after UWB transponder more easily.

REFERENCES

[1] DW1000 user manual. Version 2.05.

[2] J. Borras, P. Hatrack, and N. B. Mandayam. Decision theoretic framework for nlos identification. In Vehicular Technology Conference, 1998. VTC 98. 48th IEEE, volume 2, pages 1583-1587 vol.2, May 1998.

[3] decaWave. APS011: Sources of error in DW1000 based two-way ranging (TWR) schemes. Version 1.0.

[4] Edouard Auvinet et al. Validation of the precision of the Microsoft HoloLens augmented reality headset head and hand motion measurement. Elsevier, 2017.

[5] François Despaux, Katia Jaffrès-Runser, Adrien van den Bossche, Tierry Val. Accurate and Platform-agnostic Time-of-flight Estimation in Ultra-Wide-Band. In 27th annual IEEE International Conference on Personal, Indoor and Mobile Radio Communications (PIMRC 2016), 2016.

[6] I. Guvenc, C. C. Chong, and F. Watanabe. Nlos identification and mitigation for uwb localization systems. In 2007 IEEE Wireless Communications and Networking Conference, pages 1571-1576, March 2007.

[7] Hewlett Packard. Fundamentals of Quartz Oscillators. Application Note 200-2.

[8] IEEE Computer Society, LAN/MAN Standards Committee, Institute of Electrical and Electronics Engineers and IEEE-SA Standards Board. IEEE Standard for Information Technology – Telecommunications and Information Exchange Between Systems – Local and Metropolitan Area Networks – Specific Requirements Part 15.4: Wireless Medium Access Control (MAC) and Physical Layer (PHY) Specifications for Low-Rate Wireless Personal Area Networks (WPANs). IEEE Std 802.15.4a-2007(Amendment to IEEE Std 802.15.4-2006), pages 1-203, 2007.

[9] Jasurbek Khodjaev, Yongwan Park and Aamir Saeed Malik. Survey of NLOS identification and error mitigation problems in UWB-based positioning algorithms for dense environments. Annals of Telecommunications – annals des télécommunications, 2010.

[10] S. Marano, W. M. Gifford, H. Wymeersch, and M. Z. Win. Nlos identification and mitigation for localization based on uwb experimental data. IEEE Journal on Selected Areas in Communications, 28(7):1026-1035, September 2010.

[11] Jorge J. Moré. The Levenberg-Marquardt algorithm: Implementation and theory. In In G.A. Watson (ed.): Numerical Analysis. Dundee 1977, Lecture Notes Math. 630, 1978, S. 105-116. 1978.

[12] Nezo Ibrahim Fofana, Adrien van den Bossche, Réjane Dalcé, Thierry Val. An Original Correction Method for Indoor Ultra Wide Band Ranging-Based Localisation System. In Ad-hoc, Mobile, and Wireless Networks, 2016.

[13] J. Schroeder, S. Galler, K. Kyamakya, and K. Jobmann. Nlos detection algorithms for ultra-wideband localization. In 2007 4th Workshop on Positioning, Navigation and Communication, pages 159-166, March 2007.

[14] A. van den Bossche, R. Dalcé, I. Fofana, and T. Val. Decaduino: An open framework for wireless time-of-flight ranging systems. In 2016 Wireless Days (WD), pages 1-7, March 2016.

[15] H. Wymeersch, S. Marano, W. M. Gifford, and M. Z. Win. A machine learning approach to ranging error mitigation for uwb localization. IEEE Transactions on Communications, 60(6):1719-1728, June 2012.

[16] Lukasz Zwirello. Realization Limits of Impule-Radio UWB Indoor Localization Systems. PhD thesis, KIT, 2013.